City University of New York (CUNY)

CUNY Academic Works

2013

A Novel Biomaterial Enables Chemotactic Study of Motile Central Nervous System-derived Tumor Cells

Tanya Singh
CUNY City College

How does access to this work benefit you? Let us know!

A Novel Biomaterial Enables Chemotactic Study of Motile Central Nervous System-derived Tumor Cells

---

Thesis

Submitted in partial fulfillment of the requirement for the degree

Master of Science in Biomedical Engineering

at

The City College of New York

of the

City University of New York

By:

Tanya Singh

May 2013

Approved:

Professor Maribel Vazquez, Thesis Advisor

Professor John Tarbell, Chairman

Department of Biomedical Engineering

TABLE OF CONTENTS

ABSTRACT

The local cell microenvironment plays an important role in maintaining the dynamics of the extracellular matrix (ECM) and the cell-ECM relationship. ECM is a complex network of macromolecules with distinct mechanical and biochemical characteristics [1]. The multifaceted interactions that occur between cells and the ECM are crucial to the regulation of processes that maintain homeostasis. These mechanisms are often deregulated during cancer onset and progression, which cause the ECM to become highly disorganized, alter the cell-matrix interactions, and promote increased hypervascularity and metastasis as these components are indicative of cancer progression. Medulloblastoma (MB) is one of the most common, malignant pediatric brain tumors worldwide [61]. It is characterized by high tumor invasiveness to extraneural tissues and reoccurrence in the cerebellum after total resection [2]. In the case of MBs, the migration of cells from primary tumors to other locations, within the brain or otherwise, has been one of the most clinically challenging and poorly understood processes [3]. Thus, understanding the mechanisms that regulate MB dispersal within the central nervous system (CNS) and beyond is especially important. The migration of brain cancer cells is highly complex, involving significant interactions with ECM, and chemoattractants that either diffuse from blood vessels and/or are produced by neighboring cells [4, 5]. Understanding the cell-ECM relationship provides insight into their interactions and assists in the study of endogenous cell migratory behaviors.

In order to examine the chemotaxis of MB-derived cells, this study first examined how migration along distinct ECM affected cell migratory responses to the well-studied protein, Epidermal Growth Factor (EGF). MB phenotype and motility were examined within 7 different types of ECM Poly-D-Lysine (PDL), Matrigel, Laminin, Collagen-1, Fibronectin, a 10% blend of Laminin-Collagen1, a 20% blend of Laminin-Collagen 1 and a cellulose derived synthetic hydrogel, CMC.

The average changes in cell morphology, over time in 2D and 3D are quantified using the NIH software, ImageJ, to reveal that CMC allows for a cell-ECM relationship typically believed to present in tumors when compared to other ECMs tested. The interaction of the cells with the CMC hydrogels exhibited amoeboidal morphology that is believed to indicate the "readiness" of a cell to migrate within a given environment. Investigation of CMC hydrogels revealed a polysaccharide that enables MB chemotactic study towards EGF with minimal haptotaxis, i.e. migration induced along the ECM alone .CMC gels used as ECM thereby facilitate unique, mechanistic study of MB chemotaxis because the hydrogel itself minimizes integrin interactions between cells and the ECM. This phenomenon was observed via immunocytochemistry staining performed on the Daoy cells seeded onto CMCs. Integrin $\alpha_v\beta_3$ expression was not visualized upon CMC hydrogels when compared to C-1, MGL, and LAM coatings.

This data in this study illustrates a new application of biomaterials as in vitro test systems with which to mechanistically examine the migratory responses of cells associated with numerous central nervous system (CNS) disorders, including cancer, Parkinson's, multiple sclerosis (MS) and others. Such investigation can uniquely contribute to the generation of pharmacological compounds and migration-targeted therapies to prevent tumor dispersal in the brain and metastasis.

CHAPTER 1: INTRODUCTION

Papers showing multiple ECM with Medulloblastoma (MB):

Proteins	Number of Papers	Year
Collagen	Ranger, A et al; Liang et al; Pilorget et. al; Corcoran et al;	2010;2008;2003
Laminin	Pilorget et. al; Wikstrand, CJ et al;	2003; 1991
Fibronectin	Pilorget et. al; Wikstrand, CJ et al; Mohan, AL et al;	2003;1991; 2012
Matrigel	Zavarella, S et al; Wikstrand, CJ et al; Barthomeuf, C et al; Sterling-Levis, K and White, L.	2009;1991; 2006; 2003

We believe that the type of ECM chosen for study affects MB migration because the morphology of the MB-derived cells has shown to change with different ECMs. This will further affect how ready cells are to migrate due to the differences in the anchoring of the cells via receptor-integrin interaction between the cells and the matrix. This is important for our study because we want an ECM that does not affect migration in order to gain a better understanding towards the mechanisms involved in cell chemotaxis.

1.1 Importance of Cancer Cell Migration within ECM

The migration of cancer cells within defined ECM has garnered increasing interest among CNS researchers who examine the formation and dissemination of tumors [3, 6-8] via metastasis [3, 6, 7] and the motility of so-called cancer stem cells [1, 3]. The matrix microenvironment plays a critical role in cell migration, as cells are well known to interact with the proteins of the surrounding extracellular matrix (ECM) to achieve locomotion (reviewed in [1, 9, 10]. The stiffness and elasticity of the matrix [1], its protein composition, and chemical structure, as well as ECM fiber size, pore size and distribution [10] have all been shown to affect cell migration is meaningful ways, as seen in Figure 1. For example, matrix stiffness can determine cell fate, differentiation, and tissue function [1, 11], while ECM elasticity can influence how a cell senses and perceives external forces [12-14]. Further, ECM chemical components affect matrix-ligand and integrin-receptor interactions, which directly impact signal transduction cascades and cell to cell communication that regulate such critical processes as gene expression and transcription.
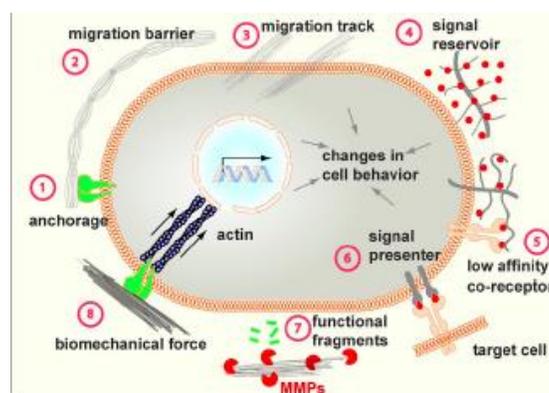

Figure1: Schematic of the Mechanisms of ECM Function. ECM function depends upon physical, biochemical, and biomechanical properties [1].

Lastly, rheological properties of the ECM, such as pore size and distribution, cross-linking, and branching modulate the transport of soluble factors within the ECM as well as the barrier function of the matrix. The barrier function may serve to block or facilitate cell migration, as the ECM can prevent or limit the diffusive range and/or accessibility of ligands to their cognate receptors [15] by binding specific growth factor signaling molecules [15-17].

1.2 Medulloblastoma Tumors

Medulloblastoma, the most common of pediatric brain cancers, occurs predominantly within the cerebellum, as shown in Figure 2, of children and frequently metastasizes to the spinal column [62]. MB is relatively rare, accounting for less than 2% of all primary brain tumors worldwide [63] and 18% of all pediatric brain tumors. More than 70% of all pediatric MBs are diagnosed in children under the age of 10. Very few occur in children younger than age 1. MB in adults is less common, but does occur and accounts for less than 1% of adult intracranial tumors [18]. With current therapies, 70-80% of children with average-risk MB survive and are free of tumors five years from diagnosis [3]. Among children with high-risk MB, 60-65% exhibit survival and no signs of tumor five years post diagnosis.
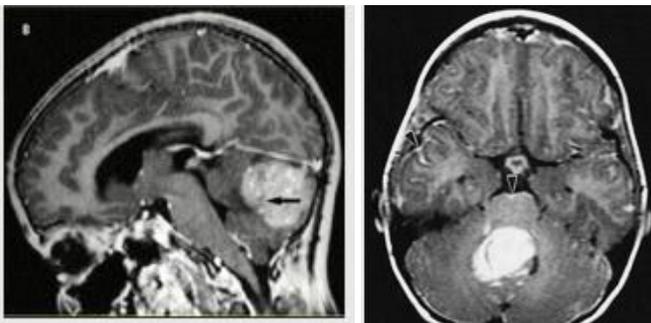

Figure 2: MRI Images of Medulloblastoma tumor originating in the cerebellum or the posterior fossa [62].

Approximately 25% of MBs originate from granule neuron precursor cells (GNPCs) after aberrant activation of the Sonic Hedgehog (Shh) pathway, Figure 3 B [3]. By contrast, glioma, the most common form of adult brain tumor, may occur across lobes and does not generally metastasize outside of the brain [19]. The current treatment options for high-risk brain tumors are associated with neural and neuroendocrine side effects, with a tremendous decline in quality of life among survivors [3], as well as growth reoccurrence and aggressive brain infiltration [3]. In the cases of gliomas and MBs, the migration of cells from primary tumors to other locations, within brain or otherwise, has been one of the most clinically challenging and poorly understood processes that contributes to the poor life prognosis of patients. This is due to highly complex interactions with the ECM, the locomotion of cancer cells is highly sensitive to stimuli from the ECM. A group of critical growth factors have been identified for their role in tumor biology and chemotaxis [20]. Overtime, secreted cytokines diffuse and generate concentration gradients that are sensed by glioma and MB-derived cells, leading to detachment and migration of these ells away from the primary tumor [21]. Deregulated ECM dynamics disrupt tissue polarity, architecture, and integrity and promote epithelial cell changes and invasion. Also, changes in ECM deviates stromal cell behavior, leading to tumor angiogenesis and inflammation by endothelial and immune cells at both primary and metastatic sites [1].
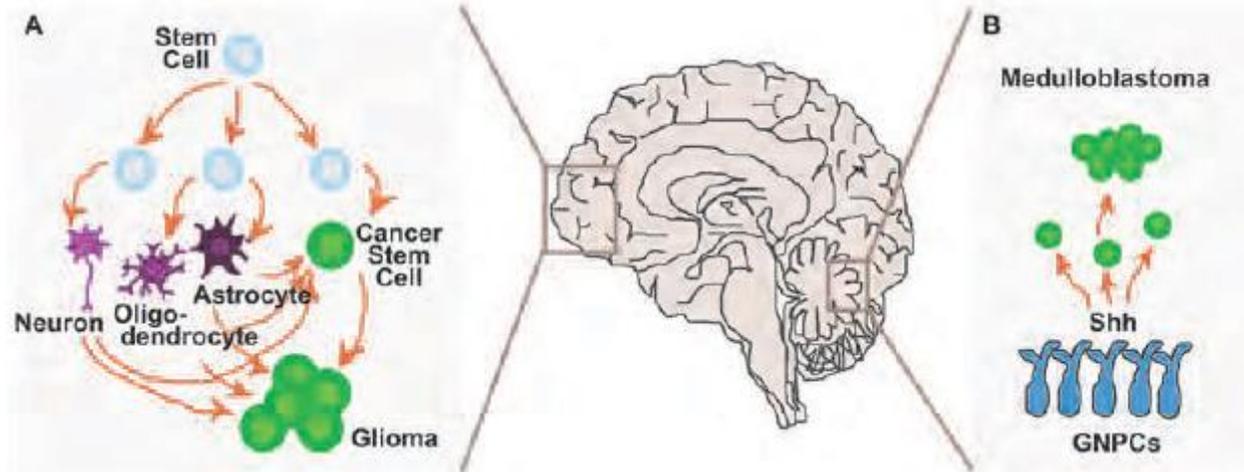
Figure 3: Schematic of the origin of brain tumors: development gone wrong. (A) During normal development, neural stem cells give rise to three main adult cell types: neurons, oligodendrocytes, and Astrocytes. Genetic alternations occur within these differentiated cells that can lead to the rise of malignant tumors. (B) Medulloblastoma cells originate in the cerebellum, from granule neuron precursor cells (GNPCs), upon un-controlled activation of Sonic Hedgehog (Shh) signaling pathway [3].

1.3 Types of ECMs for CNS Investigation

The ECM chosen for in vitro, ex vivo, and in vivo cancer study is particularly important because the ECM of the tumor environment is known to be have lower protein density [9], higher matrix stiffness [1, 22], increased hydrophobicity [23], and increased cytokine and growth factor concentrations than healthy ECM, primarily as a result of tumor hypervascularity [1, 24-26]. Further, cell-ECM dynamics change during tumor progression, as the surrounding matrix now facilitates cellular de/differentiation and becomes more porous and 'leaky' [27, 28] to facilitate metastasis, immune cell infiltration and cancer cell progression [29, 30]. Such ECM changes are particularly acute in tumors of the Central Nervous System (CNS), as ECM within brain varies greatly across anatomical regions (R), between healthy and injured brain and amid CNS tissue with different types and grades of neural tumors (reviewed in [3]. The migration of

cells derived from CNS tumors has been extensively studied in both 2D [9, 10, 31], 3D ECM models [32-34] using constituent proteins of physiological ECM found inside and outside of the CNS. These include Collagen-1 [9, 31, 35], Fibrin [10, 26], Fibronectin [9, 10], laminin [36, 37], Matrigel, hyaluronan, chitosan [26] and blends thereof. In addition, numerous researchers have developed tissue engineered materials used as ECM for clinical and surgical usage [38-43] within the CNS, such as polyacrlyamide [44] and poly(ethylene glycol) (PEG), poly(N-isopropylacrylamide) (PNIPAAm), poly-L-lysine, methylcellulose (MC), poly(lactic acid) (PLA) and pluronic F127 (an ABA block copolymer made up of poly(propylene oxide) and poly(ethylene oxide)) [26]. These hydrogels have been shown to provide several advantages in cancer treatment because they are minimally invasive [45], highly localized, and can reduce cell aggregation [26].

1.4 Haptotaxis vs. Chemotaxis

One large difficulty in the study of directed cell migration within ECM is not only the complexity of the biological process itself [1,37, 46] but also the intricate relationship between the ECM and the cellular biochemical microenvironment. Specifically, cell migration within any ECM-like material most often occurs via the two interrelated processes of haptotaxis (reviewed in [47]) and chemotaxis (reviewed in [3]). Haptotaxis is an integrin-dominated process defined as the directed movement of cells along a surface gradient of molecules, i.e. 'crawling' [3, 9]. By contrast, chemotaxis is an extracellular ligand-dominated process defined as the directed movement of cells along a concentration gradient of molecules [3, 48-50]. Tumor cells must sense a cue, most often through ligand binding, integrate signals, through activation of multiple intracellular network, and respond through modification of surrounding matrix [50]. In cancer, chemotaxis pathways can be reprogrammed in favor of tumor cell dissemination. Also, in the

11

case of metastasis, tumor cells must intravasate, extravasate and grow at a distant site [51]. Chemotaxis is thought to be involved in each of these crucial steps of tumor cell dissemination [51]. Chemotaxis is also the driving force behind coordinated cellular movement that occurs during embryogenesis, wound healing, and cancer metastasis [52].
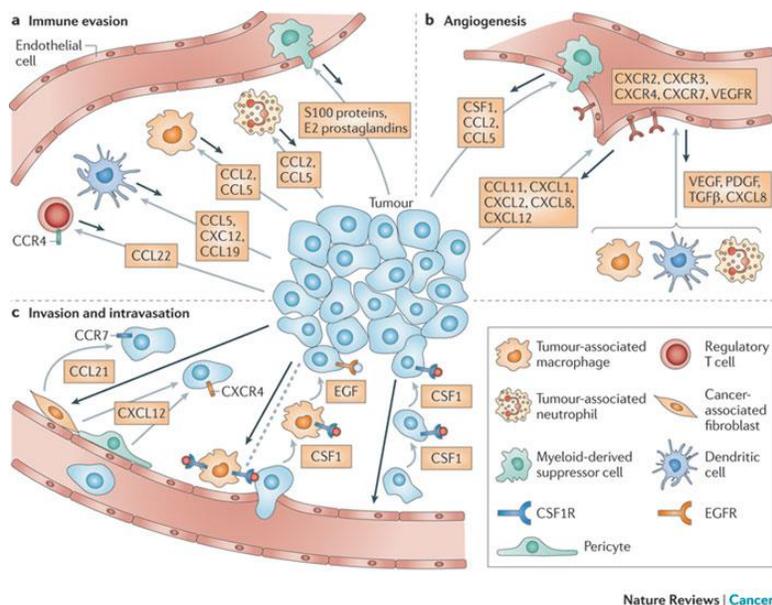
Figure 4: Schematic of the tumor microenvironment and the role of chemotaxis in the process of: immune invasion (a), angiogenesis (b), and invasion and intravasation (c) in cancer [51].

Chemotaxis is important for our investigation of MB cells because of several factors such as: metastasis of MB cells to the spinal cord, help elucidate mechanics involved in cell migration, eventual computational modeling/prediction of tumor growth and dispersion, and development of pharmacological devices. All are necessary to help explain migrational patterns via concentration gradient. This is why it is important for our investigation to find an ECM that allows for minimal cell-matrix interaction.

1.5 Microfluidic Devices

Microfluidic devices have been of great interest in the last decade and are becoming a popular bench top method of research in microfluidics. Whitesides and coworkers have revolutionized this field by developing and introducing poly dimethylsiloxane (PDMS) to the field of microfluidics. PDMS is a cross linked polymer with two components: a base and a curing agent. This PDMS solution is very viscous and can be poured into any desired mold and then hardened into an elastomeric mold. This is termed soft lithography. This technique has been utilized in our lab and has been utilized to establish concentration gradients of dextran [53] and to further investigate concentration gradients of EGF towards the chemotactic behavior of derived glia cells. Similarly, a further continuation of our study can be carried into microfluidic devices coated with ECM proteins to observe chemotactic movement of Daoy cells towards varying concentrations of EGF; EGF considered anti-migratory target.

1.6 Goals of Current Investigation

In this work we examine Carboxymethylcellulose (CMC) as a potential haptotaxis-neutral biomaterial to function as ECM for CNS tumor cell chemotaxis. CMC is a biocompatible, cellulose-derived hydrogel primarily comprised of a polysaccharide backbone with side chains of carboxy-methyl groups. CMC has recently been shown to support nucleus pulposus cell viability and to promote phenotypic matrix deposition capable of maintaining initial mechanical properties in vitro [54]. CMC is important for our investigation because the biomaterial does not degrade. CMC also allows for cell migration, but the number of cell migrating through the gel are very few.

Here we examine how CMC affects the morphology and migration of CNS-derived tumor cells compared to six other commonly used ECM. Our study examined cell responses

within: (i) Matrigel (MGL), a commercial ECM most commonly used to mimic brain; (ii) Poly-D-Lysine (PDL), the polymer used to coat tissue culture materials; (iii) Collagen-1(C-1), a primary component of mammalian ECM; (iv) Laminin (LN), a primary protein found singularly in brain; (v) Fibronectin (FN), a primary component of brain tumor ECM not readily present in healthy CNS; (vi) a blend of Collagen-1 and 10 % Laminin (CL10) (v/v) newly used for in vitro motility experiments of neurons (R); (vii) a blend of Collagen-1 and 20 % Laminin (CL20) (v/v) ; and (viii) CMC, a cellulose-based hydrogel previously unused in CNS research. Our results illustrate that the cells have the most rounded or amoeboidal phenotype measured when in contact with the CMC hydrogels when compared to the other ECM derivative proteins. Further, while most of the cells tended to migrate and aggregate towards the edges of the hydrogel, spectral analysis revealed that Daoy cells were indeed migrating through the gel, and survived for up to six days. This study is among the first to identify a biomaterial able to facilitate the study of anti-migratory chemotherapeutics for tumors of the CNS.

As the CNS ECM is well-known to change properties during tumorigenesis and dissemination, the goal of this study is to identify an ECM material with minimal cell interactions so as to enable more controlled study of the native migration patterns and motility of brain cancer cells to chemical microenvironments. This is highly impactful because anti-migratory pharmaceuticals are not currently investigated as potential chemotherapies for CNS patients since pharmacologically-induced chemotaxis is particularly affected by ECM-dependent cellular responses in the brain [55, 56].

CHAPTER 2: MATERIALS AND METHODS

2.1 Cell Culture

Medulloblastoma (MB)-derived Daoy cell line (ATCC Cat # HTB-186, Manassas, VA) was established from a tumor biopsy of a 4 year-old boy. Daoy cells were thawed, plated, and cultured in sterile Eagle minimum essential medium (EMEM) containing 9% fetal bovine serum (FBS; (Mediatech Inc., Manassas, VA), 2% L-glutamine (Mediatech Inc.) and 1% penicillin-streptomycin (Mediatech Inc.) as done previously in our lab (Dudu et al 2011). Cells were cultured (37°C, 95% humidity, 5% CO_2) and passaged (< 70% confluency) on sterile plasma-treated polystyrene tissue culture flasks (BD Biosciences, Franklin Lakes, NJ) till further use.
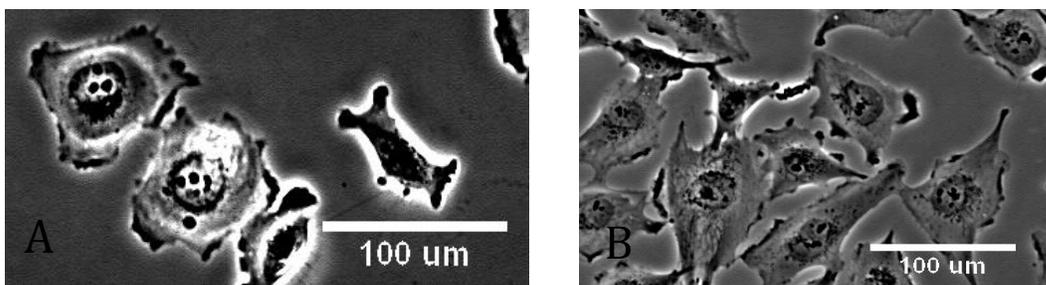

Figure 5: Phase Contrast Images of MB-derived Daoy Cells in Culture. (A) Daoy Cells in a 50% confluent flask. (B) Daoy cells in an 80% confluent flask.

2.2 Preparation of 2D and 3D Substrates for Cell Culture

The protein solutions used to coat 2D substrates were prepared as follows: PDL (Sigma-Aldrich, St, Louis, MO) solution was prepared in sterile phosphate buffered saline (1× PBS) at 100 mg/mL final concentration, added to 2-well Nunc Lab-Tek II chamber slides (Thermo Fisher Scientific, Waltham, MA) to coat overnight at room temperature, washed with PBS (phosphate buffered saline; Sigma) and dried. Fibronectin (FN) (Sigma) was diluted in PBS to 0.005% (v/v) concentration and coated on 2-well slides as described above. Growth factor-reduced Matrigel (MGL, BD Biosciences cat # 356230) was thawed at 4°C overnight and reconstituted at 100 mg/mL final concentration in sterile ice-cold PBS. Prior to use, 2-chamber slides were coated with this solution for 1 h at room temperature, solution aspirated and immediately seeded with cells. Type-1 collagen solution (C-1, rat tail-derived, 8.61 mg/mL; BD Biosciences cat # 354249, Bedford, MA) was dissolved in 0.02 N acetic acid to a final concentration of 50 mg/mL, and pH adjusted to 7.4 using 1 N NaOH. This solution was added to 2-well slides, incubated at 37°C for 1 h, washed with PBS and stored at 4°C till further use. Similarly, slides were coated with collagen-laminin (10% or 20 %, v/v) solutions, prepared by combining collagen-1 solution (50 mg/mL) with laminin (BD Biosciences, Cat # 354239, 1 mg/mL) so that the final mixture contained either 10% or 20% (v/v) laminin (CL10 or CL20, respectively). Plastic surfaces which remained uncoated with protein served as controls. Daoy cells were seeded on these substrates at a density of 1×10^4 cells/well (n = 3 wells/case) and cultured for 3 days in EMEM medium.
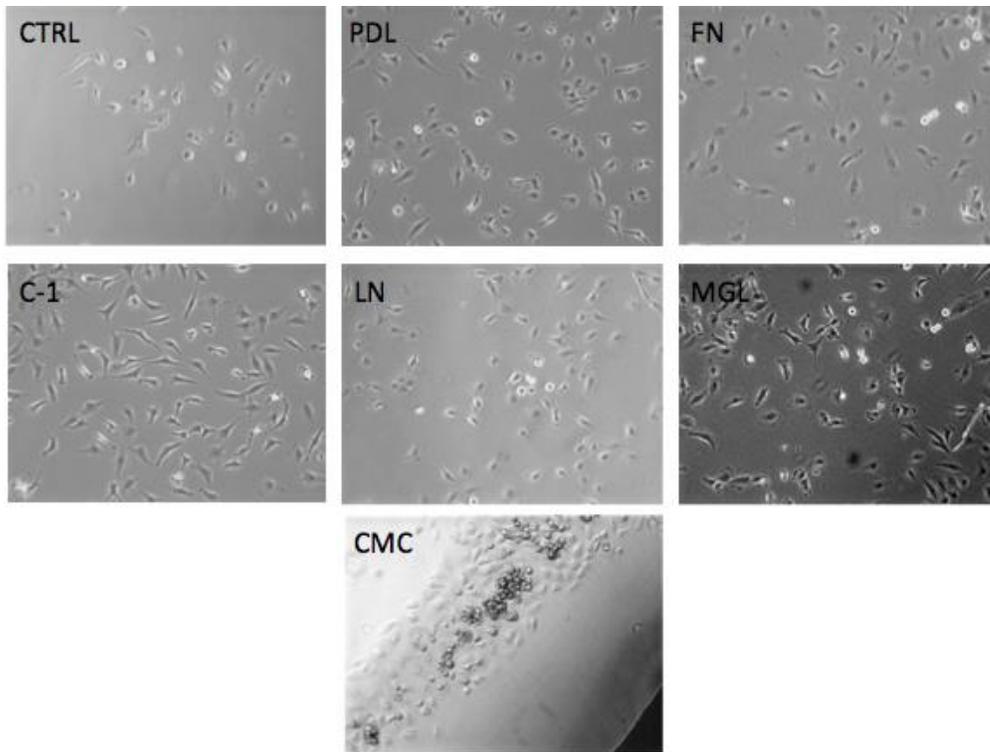
Figure 6: Phase Contrast Images of Daoy Cells Cultured on Different 2D Substrates.

Five different types of 3D hydrogel solutions were prepared. Collagen-1 solution (C-1) was reconstituted at 2 mg/mL (pH~7.4) final concentration as detailed above. Matrigel solution (MGL) was reconstituted in ice-cold PBS at 2 mg/mL concentration. Collagen-laminin gels (CL10 and CL20) were prepared by mixing 2 mg/mL collagen solution with 1 mg/mL laminin, so that the final concentration of laminin was either 10% or 20% (v/v). All the above solutions were maintained on ice till cell seeding. Daoy cells mixed in these solutions at a final concentration of 1:30 (cell: gel ratio) were seeded within 2-chamber slides, and allowed to polymerize at 37°C for 30 min in humidified chambers. EMEM medium was added to these chamber slides, and cultures maintained for 3 days with media changed after every 24 h.
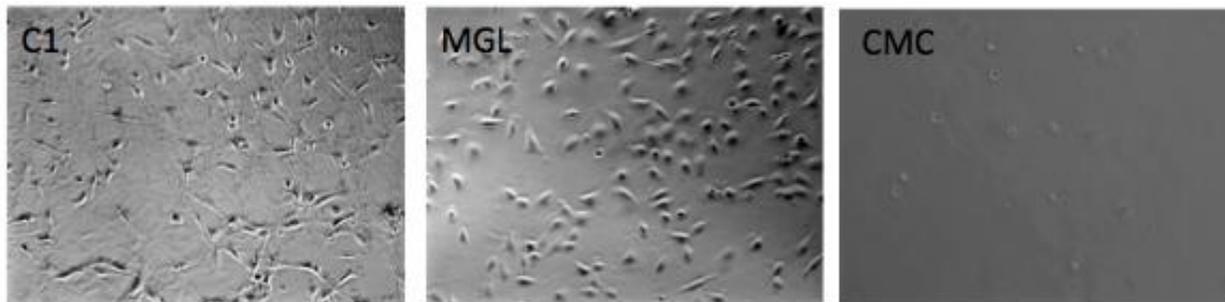
Figure 7: Phase Contrast Images of Daoy Cells Cultured of Different 3D Substrates.

Lyophilized methacrylated CMC was sterilized by a germicidal UV light exposure for 30-min before dissolving it in filter-sterilized 0.05% photoinitiator, 2-methyl-1-[4-(hydroxyethoxy)phenyl]-2-methyl-1-propanone (Irgacure 2959, I2959; Ciba Specialty Chemicals, Basel, Switzerland), in sterile Dulbecco's phosphate-buffered saline (DPBS) at 4 C to obtain a 2% (w/v). The solution was gelled between two glass slides exposed to long-wave UV light (EIKO, Shawnee, KS; peak 368 nm, 1.2 W) for 10 min to get covalently crosslinked hydrogel films· A 8mm diameter stainless steel punch was used to obtain thin hydrogel discs with a thickness of ~550um.

Since the CMC backbone is modified with methacrylate groups, which allow crosslinking, the hydrogel is formed via the production of free radicals from the photo initiator solution during photopolymerization as shown in Figure 8 below.

Figure 8: Schematic of the synthesis of methacrylated Carboxymethyl cellulose (CMC). Methacrylated CMC was synthesized through e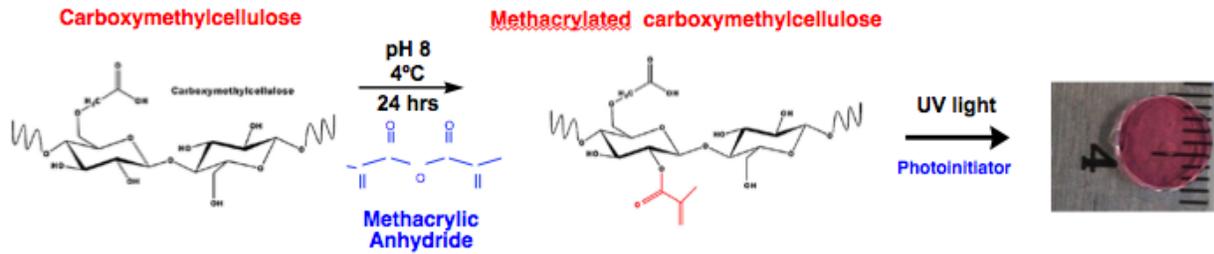sterification of hydroxyl groups via methacrylic anhydride under controlled pH and temperature. (Reza et al..2009. Biotechnology and Bioengineering. Vol. XXX, No. 9999).

2.3 Transswell Assay for Cell Migration

Transwells of 8 mm pore size (polycarbonate membranes, tissue culture treated; VWR, cat # 62406-198) were used to measure cell migration through 3D ECM as shown in Figure 2.
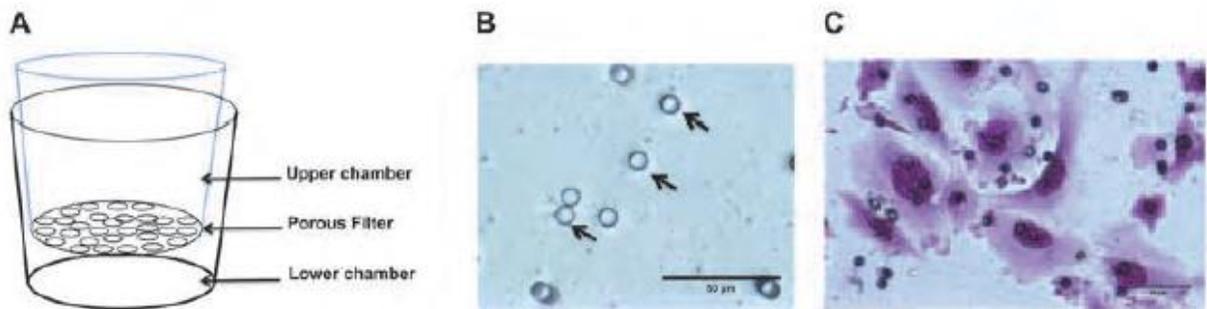
Figure 9: Boyden chamber assay. (A) Transwell migration assay are composed of a well insert with a porous filter bottom that temporarily separates the cell solution from growth factor, EGF placed in the lower chamber. (B) The filter has randomly distributed microscale diameter pores as shown by arrows. (C) Invasive Daoy cells on the underside of the filter stained and imaged for migrational analysis. Scale bar = 50μm [3].

These wells were inserted into a 24-well plate (VWR, cat # 62406-189) and utilized a 10 mm thin transparent polycarbonate membrane. Briefly, after the hydrogels were reconstituted as detailed above, 30 mL of each gel was loaded into the inserts (n = 6/case) and allowed to

polymerize (37°C, 30 min, 95% humidity). The final gel thickness in each well was ~ 0.55 mm. The inserts were placed within individual wells in a 24-well plate and 20 mL of Daoy cell solution (1×10^4 cells/mL) was seeded atop of these gels. Complete medium was added to the wells as well as the inserts to prevent gels from drying, and incubated at 37^oC with 5% CO_2 for 48 h. Cell migration across the gel and transwell was measured at two different time points of t_1= 24 h and t_2= 48 h (n = 3 wells/time point). Excess media was aspirated and the non-motile cells were removed from the upper surface of the membrane by quickly cleaning the hydrogel surface. Inserts were then rinsed in sterile PBS and stained using the Diff-Quik staining kit (Allegiance Catalog# B4132-1A) as per recommended protocols. Cell counting was performed via hemocytometer as done previously in our lab [3] by measuring cells within images of the membrane obtained at low magnification using a Nikon TE2000 inverted microscope.

2.4 MTT Cell Proliferation Assay

The Vybrant MTT Cell Proliferation Assay Kit (Invitrogen Molecular Probes, cat# V-13154, Eugene, OR) was used to determine cell viability. The MTT kit reagents: 12 mM MTT solution and SDS-HCl solution were prepared according to the provided protocol. CMC hydrogels were prepared and placed in boyden chambers in a 24 well plate, which were then seeded with MB-derived Daoy cells that were stimulated with EGF (1000ng/ml). For labeling the cells, old media from the Boyden chambers was removed and replaced with 100 μl of fresh complete culture medium.

Following this, 10 μl of the 12 mM MTT stock solution was added to all samples. The samples were incubated for 2-4 h. After incubation, 100 μl of the SDS-HCl solution was added to each well. The samples were then incubated for another 4-18 hrs. After labeling, the solution

from each well was collected and deposited into a 96 well plate- 100 µl of solution was added to each well of the 96 well plate. The plate was then inserted into a spectrophotometer, the absorbance of the solution was read at 570 nm, and compared to the control, which contained medium, MTT solution, and SDS-HCl solutions. Analysis was performed for 3 times points: 24, 48, and 72 hrs and each experiment was done in triplicate.

2.5 Imaging and Analysis

A Nikon TE2000 epi-fluorescence, inverted microscope equipped with short- and long-range objectives and a cooled CCD camera (CoolSNAP EZ, Photometrics, Tucson, AZ) was used for imaging of cells. Images were obtained in both phase-contrast and fluorescence modes (for stained cultures) and analyzed using the National Institutes of Health (NIH) ImageJ software. The projected area (A) and perimeter (P) for each cell were measured under the defined culture conditions. The average cell morphology was analyzed using the cell shape index (CSI) [57], as done previously by our group [53]:
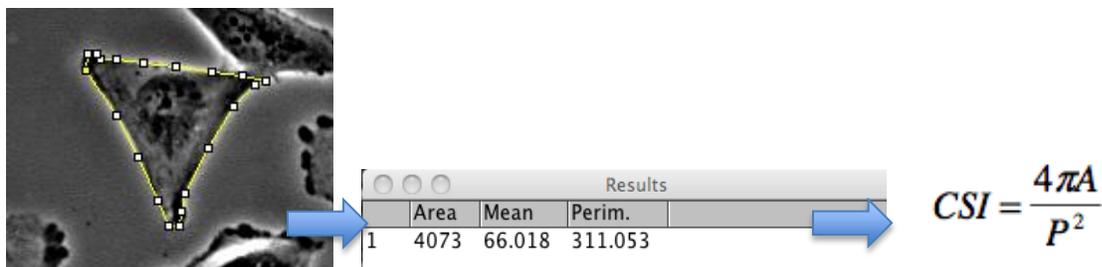
Figure 10: Schematic Showing How to Obtain Area and Perimeter Values of Daoy Cells to Solve for CSI Equation.

$$CSI = \frac{4\pi A}{P^2}$$

Statistical significance of data differences was analyzed via Student t-tests using InStat software.

2.6 Spectro-Analysis

A 24-well plate was placed under an inverted zeis microscope. A z-stack analysis was run, where the top and bottom positions/heights were standardized based on the stepper motor of the microscope. Various positions on the hydrogel were selected and 5.44 micrometer distance slices of images were obtained. The number of slices of images obtained depended on the height of the z-stack analysis. These images were then stacked to obtain a 3D image to further confirm the migration of the Daoy cells within the CMC hydrogel.

2.7 Microfluidic Device: μLane System

Figure 11: Schematic of Microfluidic Device. (A) 1st Layer of PDMS bonded to a glass slide. The two reservoirs are connected by a microchannel. (B) 2nd Layer of PDMS bonded to the first layer. A source and sink chamber align on top of the two reservoirs, and a bridged channel

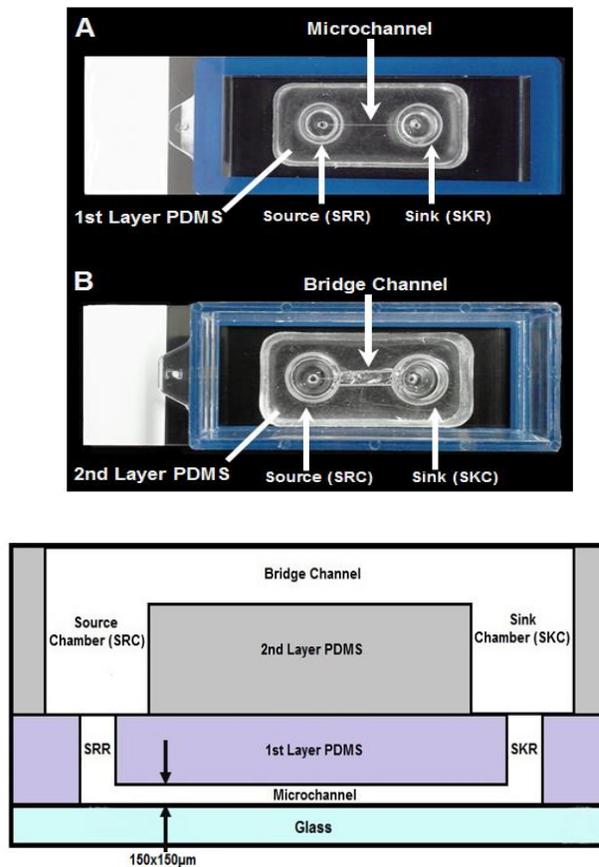connects the two chambers. (C) Schematic of the entire system, side view, showing the dimensions of the channel [Rico et al, 2013].

This study utilized our laboratory-developed µLane system, whose design and testing has been previously described [53]. The bridged µLane is fabricated via contact photolithography from elastomeric molding of two layers of polydimethylsiloxane (PDMS), which are stacked on top of one another and ozone bonded to a glass slide. The first layer includes a 150µm diameter by 15mm long microchannel, as well as a source and sink reservoir, which have volumes of 9µL each. The second layer consists of 170µL source and sink chambers, and a small hemispherical bridged channel connecting them. In order to operate, the desired diffusible reagent is placed in the source chamber, and the rest of the system is filled with PBS or media. The bridge channel precisely balances the liquid heights in the source and sink chamber, minimizing the pressure gradient between them and facilitating slow moving flow in the microchannel. This convective-diffusion is what establishes a concentration gradient between the source and the sink reservoir. The gradient can be maintained for several days, and also be modeled computationally and verified experimentally.

2.8 Immunocytochemistry (ICC) Staining

A 24 well plate was prepared with coatings of C-1 at a concentration of 2mg/ml, LN at a concentration of 1mg/ml, MGL at a concentration of 100mg/ml, and CMC at 2% v/v. Three controls were setup for this experiment. CTRl 1: Daoy cells, CTRL 2: Daoy cells cultured with antibody $\alpha_v\beta_3$ (Millipore, MAB1976X, Billerica, MA), and CTRL 3: Daoy cells cultured with Hoechst 33342 nuclear stain and antibody $\alpha_v\beta_3$. Daoy cells were seeded at a density of 5000 cells per 500 µl and incubated on substrates for ~ 2 hours. Four solutions were prepared to begin

immunostaining: 0.1%Triton X-100 in PBS, 1% blocking solution (PBSA), 1% PBS-BSA solution, and 5μg/ml of $\alpha_v\beta_3$. Cell medium was aspirated and each substrate was rinsed three times with 1X PBS. Cells were then fixed with 2-4% formalin for 10 mins. Formalin was then aspirated and the substrates were washed two times with 1X PBS for 2 mins each. Then the cells were permeablized in 0.1% Triton X in PBS for 10 mins and incubated for 60 mins with the 1% blocking solution (PBSA). After 60 mins, the substrates were washed with 1% PBS-BSA solution two times for 2 mins and were then exposed to 5μg/ml of $\alpha_v\beta_3$ and incubated overnight at 4°C. The following day the substrates were then washed two times, for two mins each, with 1X PBS. Following this CTRL 3 was exposed and incubated in Hoechst 33342 nuclear dye for 25 mins.

2.9 Statistical Analysis

One-way analysis of variance (ANOVA) was performed using Origin (version 7.5) to test for significant differences between groups. Tukey comparison was utilized to identify significant interaction between growth factor concentration and gradient. Significance level was set to $p < 0.001$.

CHAPTER 3: RESULTS

3.1 Cell-Matrix Interaction Experimental Data

The different biopolymers used as ECM for this study were chosen based on their abilities to promote cell attachment, growth, and migration. Experiments first demonstrated the time-varying differences in the Cell Shape Index, CSI, of MB cells upon 2D substrates of the ECMs chosen, as well as within 3D microenvironments generated by these ECM proteins. MB chemotaxis within 3D ECMs was next examined, followed by a spectral analysis of MB cell position within the ECMs.

Figure 12 illustrates the changes in cell shape index, CSI, of M B- cells upon 2D substrates from Day 1 to Day 3. The values of CSI for cells adhered upon 2D ECM comprised of Collagen-1, Laminin, PDL, Fibronectin, and Matrigel remained unchanged during this experimental time. By contrast, phase contrast images in Fig. 1x- Fig. 1x illustrate marked changes in cell phenotype from Day 1 to Day 3 when plated upon both Collagen-Laminin blends (10% and 20%) as ECM. The cells displayed increased elongation, In the Collagen-Laminin blends, CL10 and CL20), and Collagen-1 (C-1) as shown by phase contrast images and CSI calculations (Figure 12). Lastly, MB cells plated upon CMC gels displayed rounded morphology rather than an elongated state.
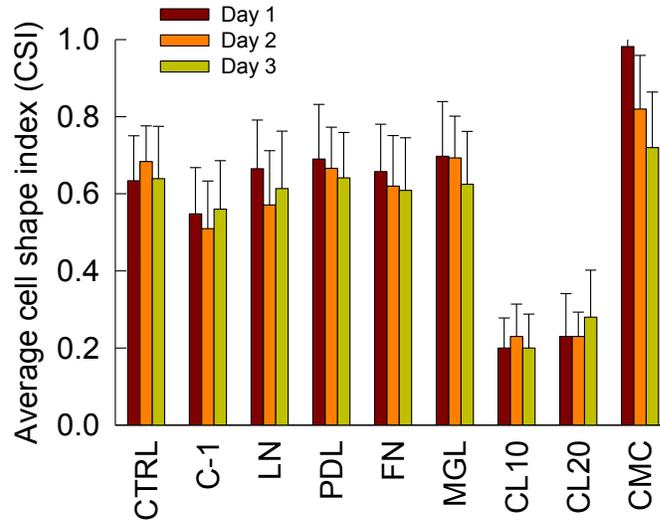
Figure 12: Changes in Average Cell shape Index (CSI) of cells cultured on 2D substrate. Measured average CSI of MB-derived cells cultured on a 2D layer of 8 different extracellular matrix (ECM) coating for 3 days: CTRL, Collagen-1, Laminin, Poly-D-Lysine, Fibronectin, Matrigel, Collagen-Laminin 10%, Collagen-Laminin 20%, and CMC. Values of statistical significance ($p < 0.05$) were measured against control conditions using culture media plates.

Figure 13 illustrates changes in CSI when MB cells were grown in 3D ECM comprised of these same biopolymers. As seen, minimal changes in CSI values from Day 1 to Day 3 was observed when using Collagen-1, Matrigel, and collagen blends as ECM. The CSI of cells within Collagen-1 3D gels was less than Matrigel, which was less than of both Collagen-Laminin blends (CL10 and CL20). CSI of cells within CMC gels were the minimal of those measured. Fluorescent image in Fig. 13 A illustrates CMC 3D hydrogels housed cells that remained in a rounded state even immediately after seeding. Also the cells immediately dispersed away from the center, which is the initial seeding placement of the cells with the pipet, of the gel towards the edges, which was observed via time-lapse microscopy.
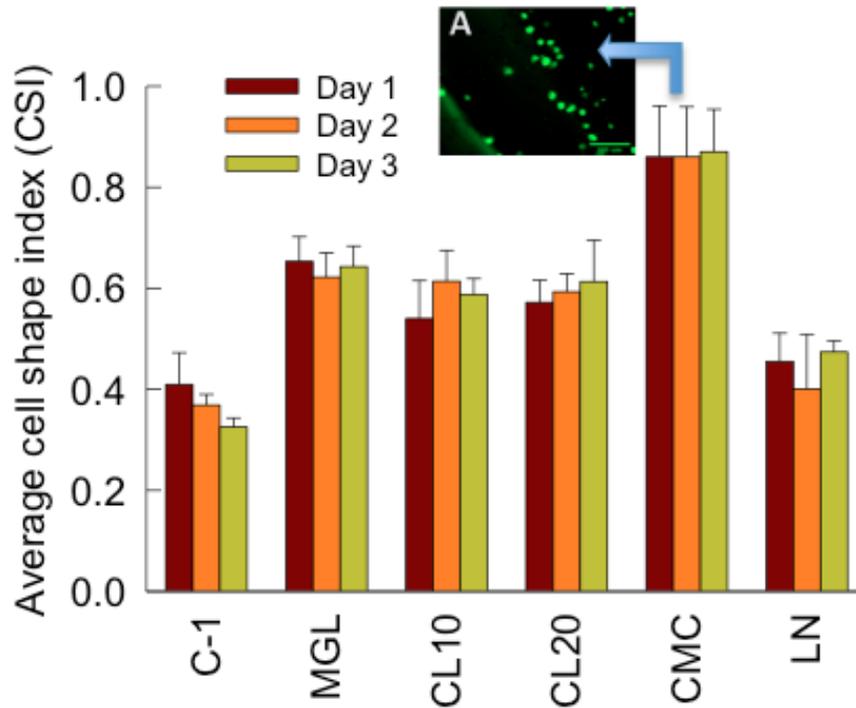
Figure 13: Changes in Average CSI of cell within 3D ECMs. Measured average CSI of MB-derived cells embedded within 3D ECM microenvironments for t = 3 days: C1, MGL, CL10, CL20, and CMC. Values of statistical significance were measured against C-1 gels held as controls for these experiments.

The next set of experiments then utilized the different ECMs to examine MB chemotactic migration towards varying concentrations of EGF. Figure 14 displays the numbers of cells that migrated through the 3D ECMs after 24 and 48 hours. As shown, MB cells migrated in largest numbers through ECMs comprised of Matrigel at both time points, whereas MB migration within Collagen-Laminin blends resulted in similar numbers. Cell migration within an ECM of Collagen-1 resulted in the lowest number of cells at both time intervals.

Figure 14: MB Cell Migration within 3D ECM in Transwell Assays. Measured number of MB cells that migrated through 3D ECM over 48 hours: C-1, MGL, CL10, and CL20.

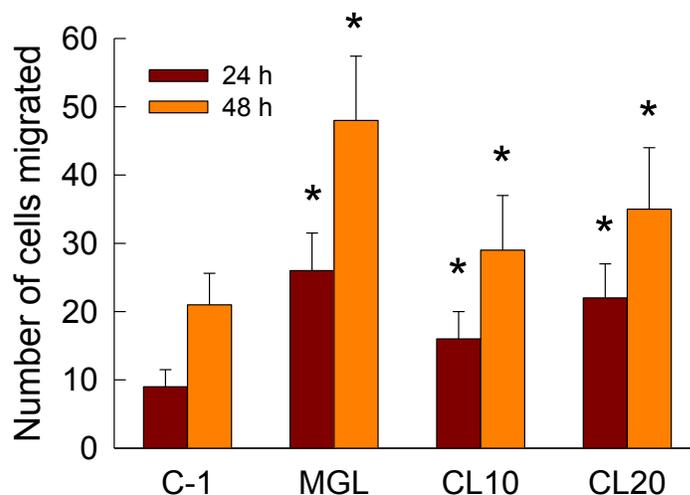As a last set of experiments, spectral analysis was performed on the 3D ECMs to estimate cell penetration within the matrix at the different time intervals. Cell migration within the 3D CMC hydrogel was measured in a transwell assay for 72 hours. The 3D CMC gels had zero cells migrate through the other side of the boyden chamber, but surprisingly the cells survived on this hydrogel. As shown, in Figure 15 A the cells were fluorescently stained with a membrane dye for live cells, most of the cells were alive after 72 hours. An MTT assay was utilized, Figure 16, to quantitatively prove cell survival within the CMC gels. In order to visualize any motility of Daoy cells on or within the hydrogels, spectral analysis was run as seen in Figure 15 B. Most interestingly, cells appeared to also migrate within the 3D ECM comprised of CMC hydrogel.

Images in Figure 15 A first illustrate how MB cells migrated towards the edges of the transwell assay at lower time points, and then unexpectedly appear to migrate through the CMC gel itself. Also a significant amount of cells do remain in the center of the gel. Figure 15 B

displays a 3D image, complied from a z-stack of 5.44-micron slices showing the Daoy cells are inside the gel.
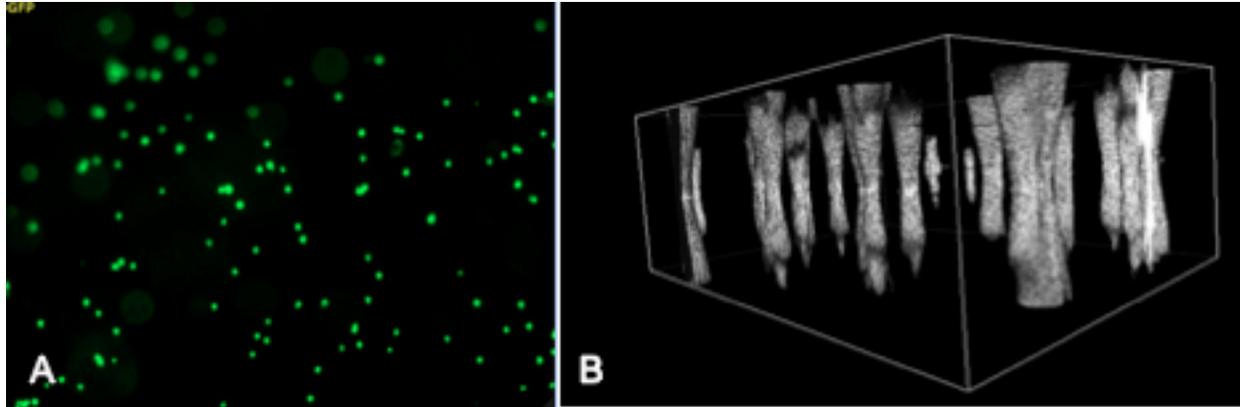
Figure 15: (A) Fluorescent Daoy cells on top of the CMC hydrogel (B) Spectral analysis of MB derived cells within CMC 3D hydrogel after 72 hours.

Finally in order to determine the cell viability of Daoy cells within/on the CMC hydrogels quantitatively, an MTT assay was performed. The cells were seeded on top of the CMC hydrogels and exposed to EGF at three different time points: 1d, 2d, 3d. Figure 16 graph displays the results of the assay. After 3d, Daoy cells appear to have proliferated/ have linear growth within/on the CMC hydrogels. Thus the CMC hydrogels support/promote cell growth.
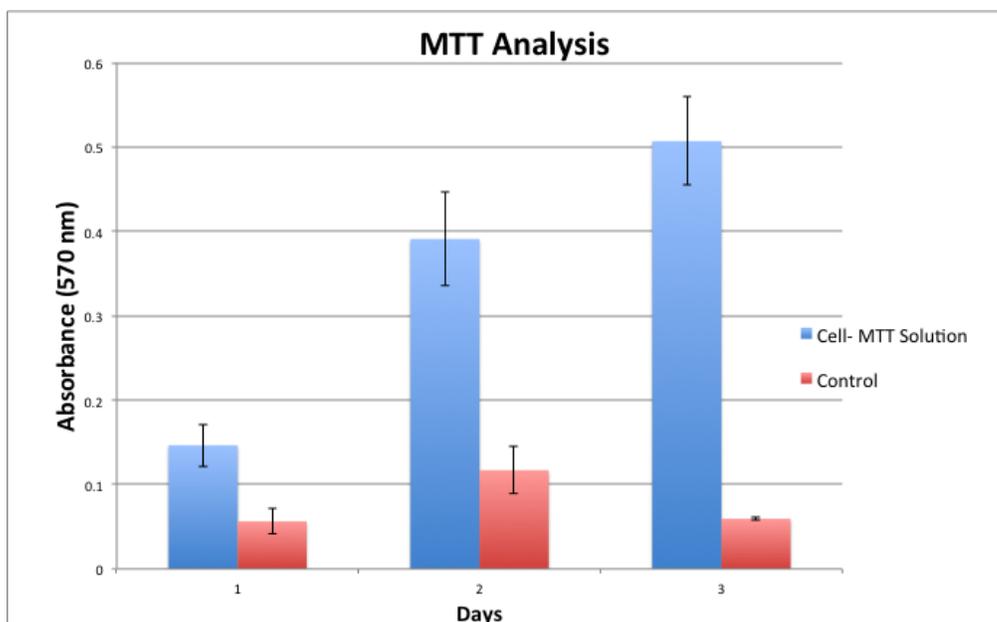
Figure 16: MTT assay analysis showing the absorbance of the cell-MTT/SDS solution using a spectrophotometer to determine cell viability.

To quantitatively prove that CMC hydrogels indeed provide for a chemotactic migration of MB-derived Daoy cells and that Daoy cells have minimal integrin-receptor interaction with the CMC hydrogel, ICC was performed. As can be seen from Figure 17, integrin-receptor interaction is much higher in C-1, MGL, and LAM ECM coatings than with the CMC hydrogels. The expression of the integrin on C-1, MGL, and LAM are consistently around the nucleus whereas for the CMC hydrogels, integrin expression in limited to one side of the nucleus. This phenomenon can be attributed/is due to the cell spreading/elongation of MB derived on the C-1, MGL, and LAM matrices. Another factor could be the presence of growth factors secreted by the cells when in contact with the ECM proteins as control images (not shown in figure below): Daoy cells seeded onto 24 well plates without the exposure to any ECM proteins also exhibited similar effects as the CMC hydrogels, where the expression of integrin $\alpha_v\beta_3$ was very minimal or the expression of $\alpha_v\beta_3$ integrin was not observed. Qualitatively, phase contrast images (not

shown) of the fixed Daoy cells, shows cell extension in C-1, MGL, and LAM matrices, but

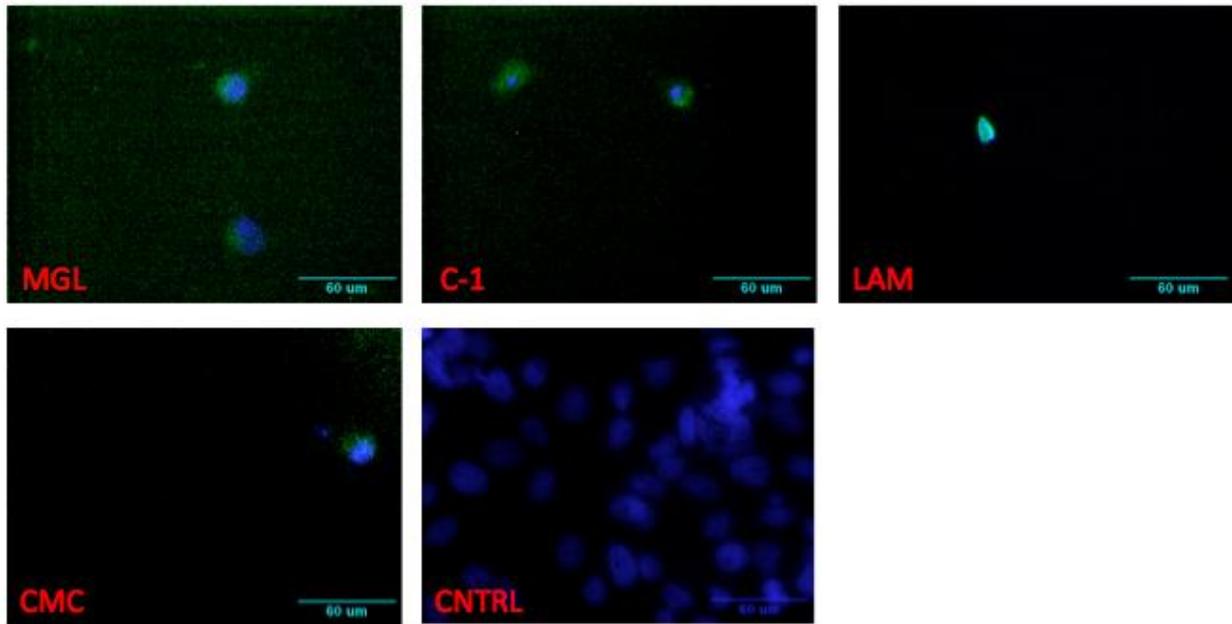amoeboidal morphology of cells in CMC hydrogels.

Figure 17: Immunocytochemistry Staining of Daoy Cells with Integrin $\alpha_v\beta_3$ on different ECM proteins and CMC hydrogel. CNTRL: Daoy cells cultured on tissue culture treated 24 well plate, fixed and exposed to Hoechst 33342 nuclear dye.

CHAPTER 4: DISCUSSION

The migration of cells from pediatric brain tumors has been largely understudied despite their high tumor metastatic potential and aggressive invasion into healthy brain [3]. While interactions between cells and ECM proteins have been widely studied, the migrational behavior of MB cells within synthetic hydrogels is largely unknown. The current study examined morphological changes and migrational behavior of MB cells within 7 different types of ECM compounds, and a cell plant wall derived hydrogel CMC. CMC seeded cells were exposed an EGF concentration of 1000 ng/ml, previously established by Dudu et. al, 2011 , to be chemoattractive to MB.

Initial 2D seeded substrates displayed that the CMC gels change the cells into an ameoboidal shape rather than an elongated shape. No statistical difference in morphology was observed between CTRL, C-1, LN, PDL, FN, and MGL. Collagen-laminin blends displayed significantly different morphology compared to other substrates. Significant cell elongation on the substrate was observed. This data suggest that the 2D substrates tested herein promote cell crawling. CMC was the only substrate that consistently displayed high levels of amoeboidal shaped Daoy cells on all three days. This phenomenon may be attributed to the amount the of integrin interaction between the cells and the ECM.

Similar effects were seen in the CSI of cells seeded onto 3D substrates. To examine the affects of ECM proteins on the migration of Daoy cells, the cells were exposed to an optimal concentration of EGF (1000ng/ml) for chemotactic migration. As displayed in Figure 6, Matrigel attracted the largest number of cells at both time points: 24h and 48 h. The CMC hydrogels were also tested by producing 8 mm hydrogel disks which were placed within boyden

chambers and seeded with membrane fluorescent cells. The penetration of the Daoy cells was observed via compilation of 5.44 micron sliced images in a z-stack.

The data from the CSI and migrational experiments together reveal that the CMC hydrogels allow for the chemotactic study of MB-derived Daoy cells enabling minimal haptotactic migration which is indicated by the ameoboidal shape of the Daoy cells. Also the ameoboidal morphology exhibited by the cells is indicative to the ready-ness of a cell to migrate within a given environment. Since the mechanics behind the migration of brain cancer cells are still not completely understood. This study will help elucidate the mechanisms that may be involved in the chemotactic migration of MB-derived Daoy cells. MB cells exhibit different morphology on different substrates. This phenomenon is due to the dependence of the cell-ECM integrin-receptor relationship. Also, the migration of the MB cells along the ECM via chemotaxis or haptotaxis.

Chemotactic migration toward EGF was tested with C-1, MGL, CL10, and CL-20 ECMs. In previous studies, EGF has been shown to be an anti-migratory target [58, 59] and such is supported by our study/data. In Figure 14, increased migration was observed through MGL than the other substrates. But this could be due to different growth factors present/make up MGL that the other substrates lacked.

MB cells survived on/within CMCs for greater than three days. CMC, previously believed not to sustain cell viability with increasing stiffness [54]. This formulation of cellulose has not been tested as a CNS matrix for MB migration. As our data suggests, CMC indeed provides low integrin interaction with the MB cells highlighting the chemotactic migration of

these cells. This phenomenon is in large due to the anchorage-independent proliferative ability of cancer cells.

Cancer cells have reduced requirements for substratum adhesion and are able to survive and grown under nonadhesive or anchorage-independent condition by inhibiting anoikis-related apoptotic pathways. This ability of cancer cells gives them outstanding properties for uncontrolled growth and metastisis [60]. Metastasis requires cancer cells to detach and migrate away from the primary tumor, by definition. Cancer cells then intravasate into the blood and lymphatic vessels. This migratory response and ability to survive without anchorage-dependence gives cancer cells their metastatic potential. Inhibiting this ability of cancer cells would in turn prevent metastasis. CMC hydrogels provide a similar anchorage-independent niche for cancer cells allowing researchers to manipulate this platform for anti-therapeutic drug treatments for cancer patients.

Thus far, the low integrin interaction of the Daoy cells with the CMC hydrogels highlights a chemotactic migratory response. Such a hydrogel reduces the dependence of cells on ECMs for migration. Further allowing testing of cell migration behavior to chemical changes and therapeutic testing for anti-migratory drugs.

CHAPTER 5: CONCLUSION

The current study demonstrates that the CMC hydrogels, in comparison to the other ECM proteins tested, helps provide a natural migratory pattern for the Daoy cells. The results support that CMC hydrogels promote a haptotactic neutral matrix even in the presence of chemokines. These hydrogels could be utilized for the manipulation/ testing of pharmacological drugs to inhibit migration of cancer cells- preventing metastasis.

5.1 Future Work

Continued studies will utilize microfluidic devices to investigate the migration of Daoy cells within a concentration gradient dependent environment. Further examination of the CMC hydrogels via testing it as a matrix for the co-culture of neural, endothelial, and possibly glia cells. As well as observing migration of the co-cultured cells within the CMC hydrogels. Another avenue we want to continue to explore is the integrin-receptor relationship that is displayed when the Daoy cells are exposed to the CMC hydrogels. Also, looking to see if integrin expression is dependent on chemokines/attractants within the CMC hydrogels.

REFERENCES:

1. Lu, P., V.M. Weaver, and Z. Werb, *The extracellular matrix: a dynamic niche in cancer progression.* J Cell Biol, 2012. **196**(4): p. 395-406.
2. Dhall, G., *Medulloblastoma.* J Child Neurol, 2009. **24**(11): p. 1418-30.
3. Richard A. Able, J., Veronica Dudu, and Maribel Vazquez, *<Migration & Invasion of Brain Tumor.pdf>.* Glioma- Exploring Its Biology and Practical Relevance, ed. A. Ghosh2011, Croatia: InTech. 498.
4. Condeelis, J. and J.E. Segall, *Intravital imaging of cell movement in tumours.* Nat Rev Cancer, 2003. **3**(12): p. 921-30.
5. Sahai, E., *Mechanisms of cancer cell invasion.* Curr Opin Genet Dev, 2005. **15**(1): p. 87-96.
6. Liotta, L.A., *Tumor invasion and metastases--role of the extracellular matrix: Rhoads Memorial Award lecture.* Cancer Res, 1986. **46**(1): p. 1-7.
7. Kim, Y., M.A. Stolarska, and H.G. Othmer, *The role of the microenvironment in tumor growth and invasion.* Prog Biophys Mol Biol, 2011. **106**(2): p. 353-79.
8. Pupa, S.M., et al., *New insights into the role of extracellular matrix during tumor onset and progression.* J Cell Physiol, 2002. **192**(3): p. 259-67.
9. Berrier, A.L. and K.M. Yamada, *Cell-matrix adhesion.* J Cell Physiol, 2007. **213**(3): p. 565-73.
10. Zaman, M.H., et al., *Migration of tumor cells in 3D matrices is governed by matrix stiffness along with cell-matrix adhesion and proteolysis.* Proc Natl Acad Sci U S A, 2006. **103**(29): p. 10889-94.
11. Wozniak, M.A., et al., *ROCK-generated contractility regulates breast epithelial cell differentiation in response to the physical properties of a three-dimensional collagen matrix.* J Cell Biol, 2003. **163**(3): p. 583-95.
12. Gehler, S., et al., *Filamin A-beta1 integrin complex tunes epithelial cell response to matrix tension.* Mol Biol Cell, 2009. **20**(14): p. 3224-38.
13. Lopez, J.I., J.K. Mouw, and V.M. Weaver, *Biomechanical regulation of cell orientation and fate.* Oncogene, 2008. **27**(55): p. 6981-93.
14. Paszek, M.J., et al., *Tensional homeostasis and the malignant phenotype.* Cancer Cell, 2005. **8**(3): p. 241-54.
15. Norton, W.H., et al., *HSPG synthesis by zebrafish Ext2 and Extl3 is required for Fgf10 signalling during limb development.* Development, 2005. **132**(22): p. 4963-73.
16. Hynes, R.O., *The extracellular matrix: not just pretty fibrils.* Science, 2009. **326**(5957): p. 1216-9.
17. Lu, P., et al., *Extracellular matrix degradation and remodeling in development and disease.* Cold Spring Harb Perspect Biol, 2011. **3**(12).
18. Lai, R., *Survival of patients with adult medulloblastoma: a population-based study.* Cancer, 2008. **112**(7): p. 1568-74.
19. Lassman, A.B., *Molecular biology of gliomas.* Curr Neurol Neurosci Rep, 2004. **4**(3): p. 228-33.
20. Hamel, W. and M. Westphal, *Growth factors in gliomas revisited.* Acta Neurochir (Wien), 2000. **142**(2): p. 113-37; discussion 137-8.

21.   Chicoine, M.R. and D.L. Silbergeld, *Mitogens as motogens.* J Neurooncol, 1997. **35**(3): p. 249-57.
22.   Egeblad, M., M.G. Rasch, and V.M. Weaver, *Dynamic interplay between the collagen scaffold and tumor evolution.* Curr Opin Cell Biol, 2010. **22**(5): p. 697-706.
23.   Ma, H.L., et al., *Multicellular tumor spheroids as an in vivo-like tumor model for three-dimensional imaging of chemotherapeutic and nano material cellular penetration.* Mol Imaging, 2012. **11**(6): p. 487-98.
24.   Bignon, M., et al., *Lysyl oxidase-like protein-2 regulates sprouting angiogenesis and type IV collagen assembly in the endothelial basement membrane.* Blood, 2011. **118**(14): p. 3979-89.
25.   Davis, G.E. and D.R. Senger, *Endothelial extracellular matrix: biosynthesis, remodeling, and functions during vascular morphogenesis and neovessel stabilization.* Circ Res, 2005. **97**(11): p. 1093-107.
26.   Pakulska, M.M., B.G. Ballios, and M.S. Shoichet, *Injectable hydrogels for central nervous system therapy.* Biomed Mater, 2012. **7**(2): p. 024101.
27.   Hashizume, H., et al., *Openings between defective endothelial cells explain tumor vessel leakiness.* Am J Pathol, 2000. **156**(4): p. 1363-80.
28.   Hewitt, R.E., et al., *Laminin and collagen IV subunit distribution in normal and neoplastic tissues of colorectum and breast.* Br J Cancer, 1997. **75**(2): p. 221-9.
29.   Egeblad, M., E.S. Nakasone, and Z. Werb, *Tumors as organs: complex tissues that interface with the entire organism.* Dev Cell, 2010. **18**(6): p. 884-901.
30.   Ruoslahti, E., *Specialization of tumour vasculature.* Nat Rev Cancer, 2002. **2**(2): p. 83-90.
31.   Baker, B.M. and C.S. Chen, *Deconstructing the third dimension: how 3D culture microenvironments alter cellular cues.* J Cell Sci, 2012. **125**(Pt 13): p. 3015-24.
32.   Carragher, N.O., *Profiling distinct mechanisms of tumour invasion for drug discovery: imaging adhesion, signalling and matrix turnover.* Clin Exp Metastasis, 2009. **26**(4): p. 381-97.
33.   Nyga, A., U. Cheema, and M. Loizidou, *3D tumour models: novel in vitro approaches to cancer studies.* J Cell Commun Signal, 2011. **5**(3): p. 239-48.
34.   Simao, D., et al., *Towards human central nervous system in vitro models for preclinical research: strategies for 3D neural cell culture.* BMC Proc, 2011. **5 Suppl 8**: p. P53.
35.   Smalley, K.S., M. Lioni, and M. Herlyn, *Life isn't flat: taking cancer biology to the next dimension.* In Vitro Cell Dev Biol Anim, 2006. **42**(8-9): p. 242-7.
36.   Ljubimova, J.Y., et al., *Changes in laminin isoforms associated with brain tumor invasion and angiogenesis.* Front Biosci, 2006. **11**: p. 81-8.
37.   Friedl, P. and E.B. Brocker, *The biology of cell locomotion within three-dimensional extracellular matrix.* Cell Mol Life Sci, 2000. **57**(1): p. 41-64.
38.   Cho, Y. and R.B. Borgens, *Polymer and nano-technology applications for repair and reconstruction of the central nervous system.* Exp Neurol, 2012. **233**(1): p. 126-44.
39.   Kasoju, N. and U. Bora, *Silk fibroin in tissue engineering.* Adv Healthc Mater, 2012. **1**(4): p. 393-412.
40.   Lee, S.J. and A. Atala, *Scaffold technologies for controlling cell behavior in tissue engineering.* Biomed Mater, 2013. **8**(1): p. 010201.

41.   Ozeki, T., et al., *Combination therapy of surgical tumor resection with implantation of a hydrogel containing camptothecin-loaded poly(lactic-co-glycolic acid) microspheres in a C6 rat glioma model.* Biol Pharm Bull, 2012. **35**(4): p. 545-50.

42.   Woerly, S., *Restorative surgery of the central nervous system by means of tissue engineering using NeuroGel implants.* Neurosurg Rev, 2000. **23**(2): p. 59-77; discussion 78-9.

43.   Wolf, K. and P. Friedl, *Extracellular matrix determinants of proteolytic and non-proteolytic cell migration.* Trends Cell Biol, 2011. **21**(12): p. 736-44.

44.   Ulrich, T.A., E.M. de Juan Pardo, and S. Kumar, *The mechanical rigidity of the extracellular matrix regulates the structure, motility, and proliferation of glioma cells.* Cancer Res, 2009. **69**(10): p. 4167-74.

45.   Whittemore, S.R., et al., *Optimizing stem cell grafting into the CNS.* Methods Mol Biol, 2008. **438**: p. 375-82.

46.   Even-Ram, S. and K.M. Yamada, *Cell migration in 3D matrix.* Curr Opin Cell Biol, 2005. **17**(5): p. 524-32.

47.   Dickinson, R.B. and R.T. Tranquillo, *A stochastic model for adhesion-mediated cell random motility and haptotaxis.* J Math Biol, 1993. **31**(6): p. 563-600.

48.   Lee, M.R. and T.J. Jeon, *Cell migration: regulation of cytoskeleton by Rap1 in Dictyostelium discoideum.* J Microbiol, 2012. **50**(4): p. 555-61.

49.   Servais, C. and N. Erez, *From sentinel cells to inflammatory culprits: cancer-associated fibroblasts in tumour-related inflammation.* J Pathol, 2013. **229**(2): p. 198-207.

50.   Hughes-Alford, S.K. and D.A. Lauffenburger, *Quantitative analysis of gradient sensing: towards building predictive models of chemotaxis in cancer.* Curr Opin Cell Biol, 2012. **24**(2): p. 284-91.

51.   Roussos, E.T., J.S. Condeelis, and A. Patsialou, *Chemotaxis in cancer.* Nat Rev Cancer, 2011. **11**(8): p. 573-87.

52.   Van Haastert, P.J. and P.N. Devreotes, *Chemotaxis: signalling the way forward.* Nat Rev Mol Cell Biol, 2004. **5**(8): p. 626-34.

53.   Kong, Q., et al., *A microfluidic device to establish concentration gradients using reagent density differences.* J Biomech Eng, 2010. **132**(12): p. 121012.

54.   Reza, A.T. and S.B. Nicoll, *Characterization of novel photocrosslinked carboxymethylcellulose hydrogels for encapsulation of nucleus pulposus cells.* Acta Biomater, 2010. **6**(1): p. 179-86.

55.   Decaestecker, C., et al., *Can anti-migratory drugs be screened in vitro? A review of 2D and 3D assays for the quantitative analysis of cell migration.* Med Res Rev, 2007. **27**(2): p. 149-76.

56.   Millerot-Serrurot, E., et al., *3D collagen type I matrix inhibits the antimigratory effect of doxorubicin.* Cancer Cell Int, 2010. **10**: p. 26.

57.   Shen, J.Y., et al., *Three-dimensional microchannels in biodegradable polymeric films for control orientation and phenotype of vascular smooth muscle cells.* Tissue Eng, 2006. **12**(8): p. 2229-40.

58.   Dudu, V., V. Rotari, and M. Vazquez, *Targeted extracellular nanoparticles enable intracellular detection of activated epidermal growth factor receptor in living brain cancer cells.* Nanomedicine, 2011. **7**(6): p. 896-903.

59. Dudu, V., V. Rotari, and M. Vazquez, *Sendai virus-based liposomes enable targeted cytosolic delivery of nanoparticles in brain tumor-derived cells.* J Nanobiotechnology, 2012. **10**: p. 9.
60. Wang, L.H., *Molecular signaling regulating anchorage-independent growth of cancer cells.* Mt Sinai J Med, 2004. **71**(6): p. 361-7.